iScience, Volume *24*

Supplemental Information

A design principle for posttranslational chaotic oscillators

Hiroto Q. Yamaguchi, Koji L. Ode, and Hiroki R. Ueda

Supplemental Figures

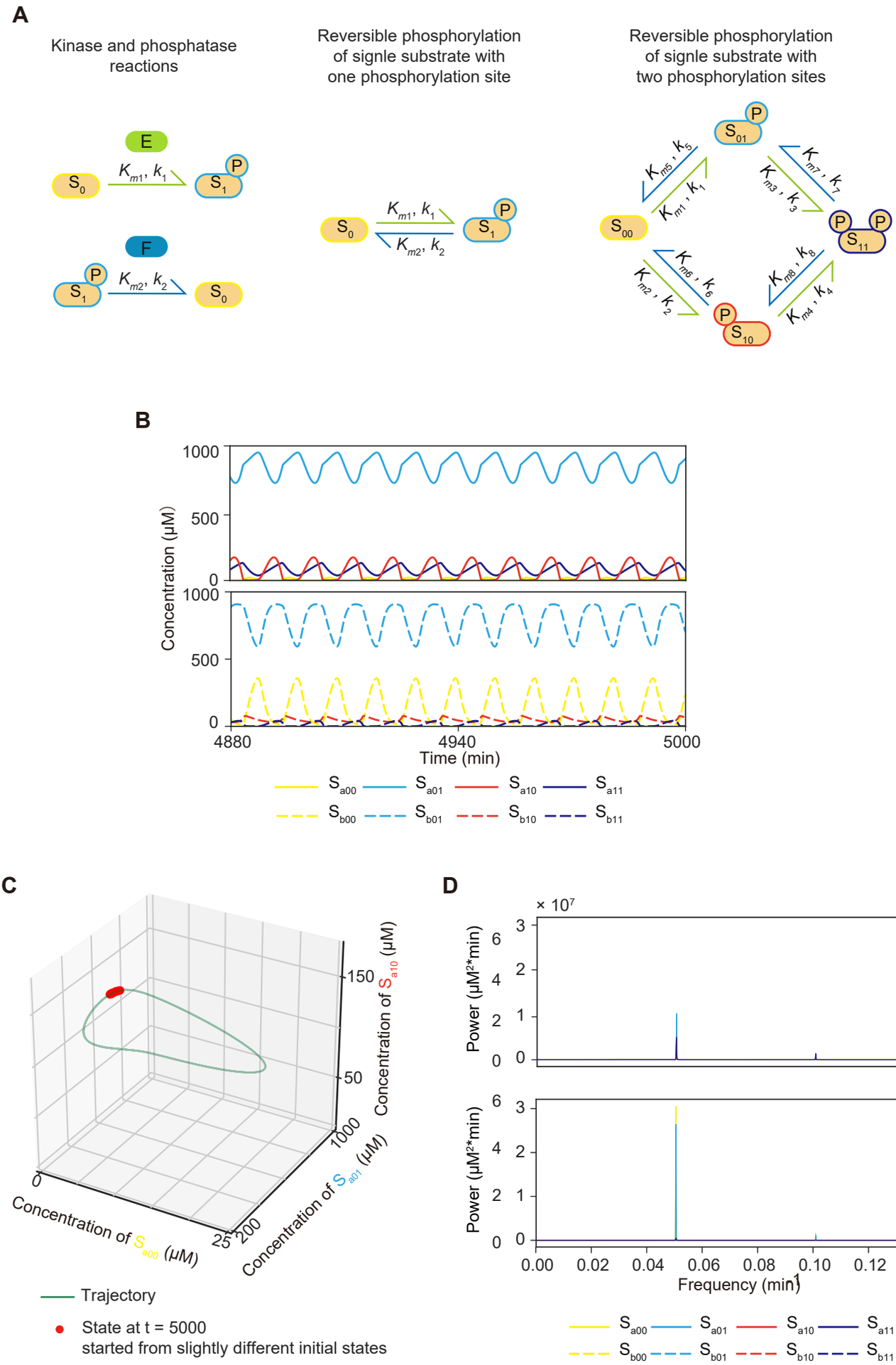

Figure S1. Yamaguchi et al.

Figure S1. Oscillatory behavior of a coupled dual-phosphorylation system

(A) Scheme of reversible phosphorylation models.

(B) An example time course of oscillatory phosphorylation dynamics.

(C) The example oscillatory dynamics of t = 0 min to t = 5,000 min are projected to S_{a00}-S_{a01}-S_{a10} space (green line). Red dots indicate the phosphorylation states at t = 5,000 min obtained from 200 runs of the simulation with slightly different initial conditions.

(D) Power spectrum of the example oscillatory trajectory analyzed by FFT.

See also **Figure 1**.

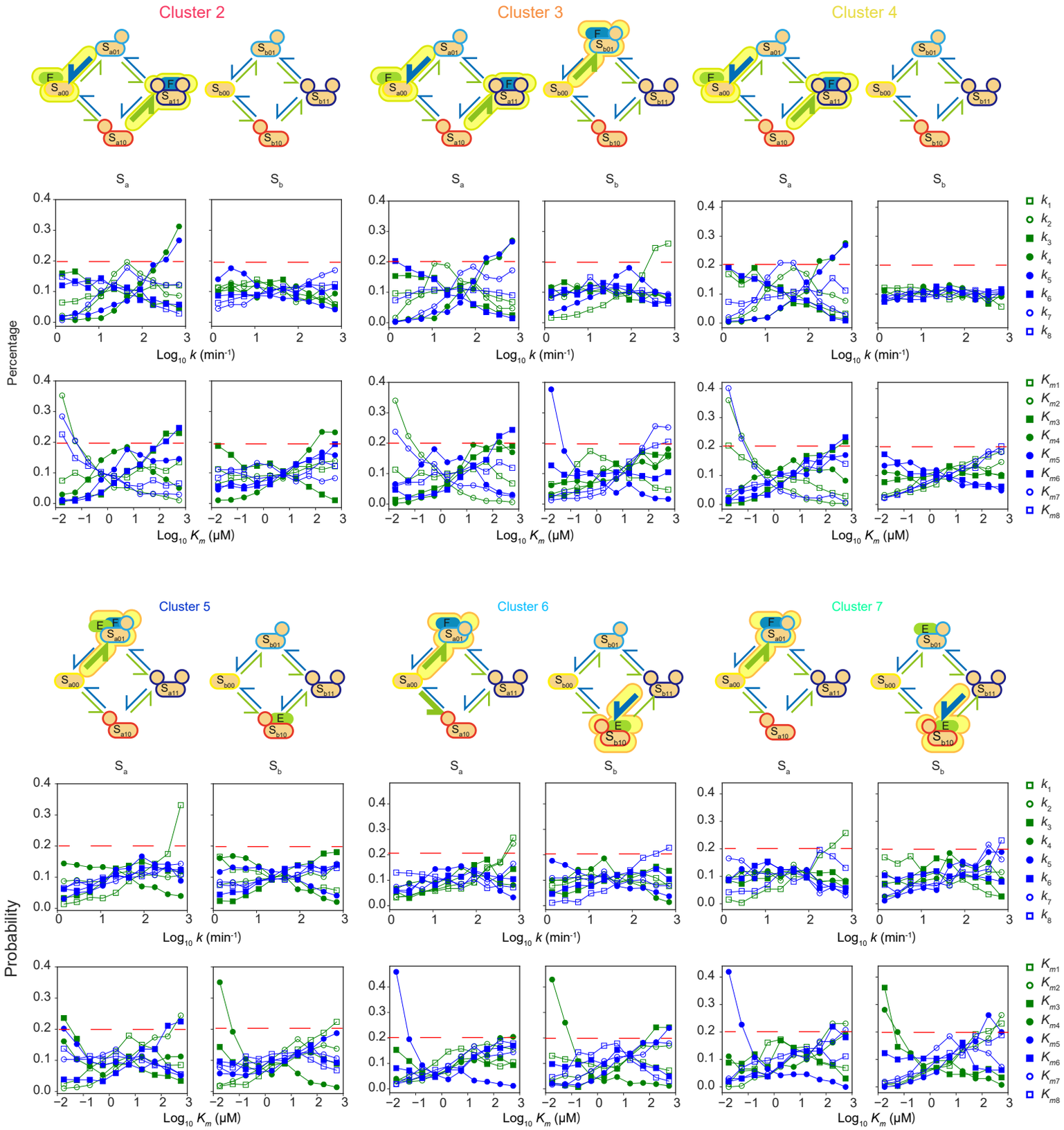

Figure S2. Yamaguchi et al.

Figure S2. Parameter motifs found in chaotic parameter sets

Schematic representation and parameter histograms of the chaotic parameter clusters shown in the same manner as in **Figure 2**.

See also **Figure 2**.

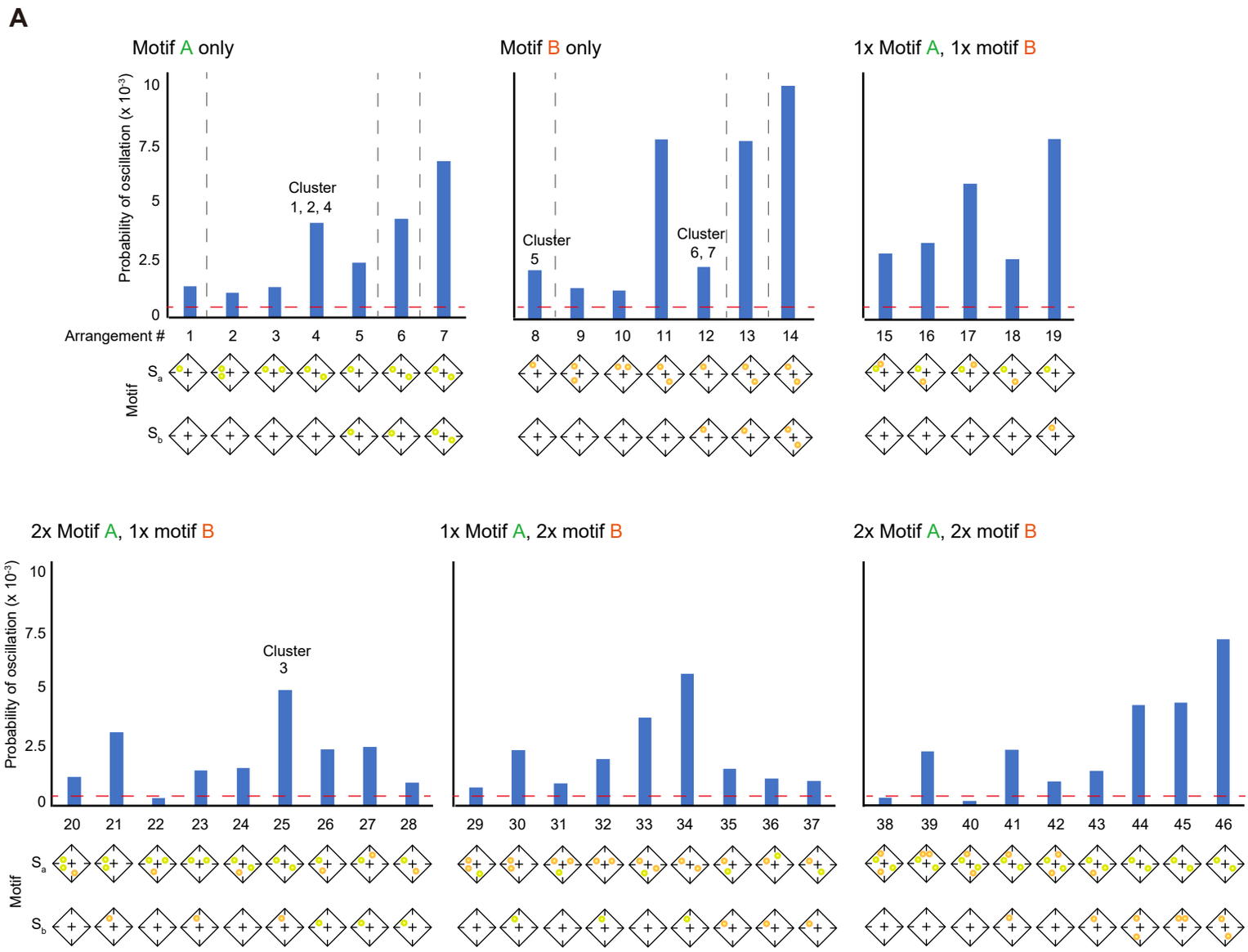

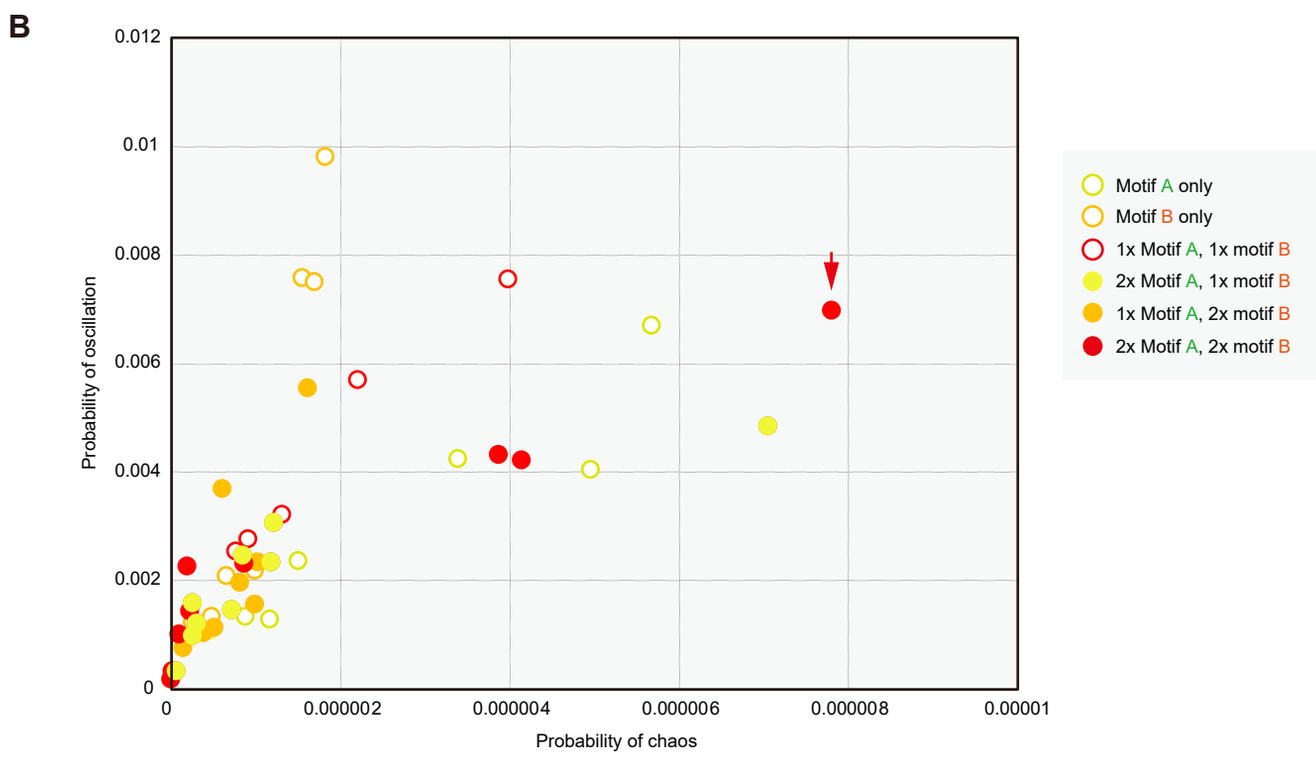

Figure S3. Yamaguchi et al.

Figure S3. Specific arrangements of motif structure are important for chaos generation

(A) Bar charts indicate the probability of oscillatory parameter sets found in the presence of each imposed motif. Imposed motif arrangements are shown in the same manner as in **Figure 3**.

(B) A comparison of the probability of chaos behavior and oscillation for parameters in the presence of each combination of imposed motifs. The red arrow indicates the motif arrangement with the highest probability of chaos behavior (i.e., arrangement #46).

See also **Figure 3**.

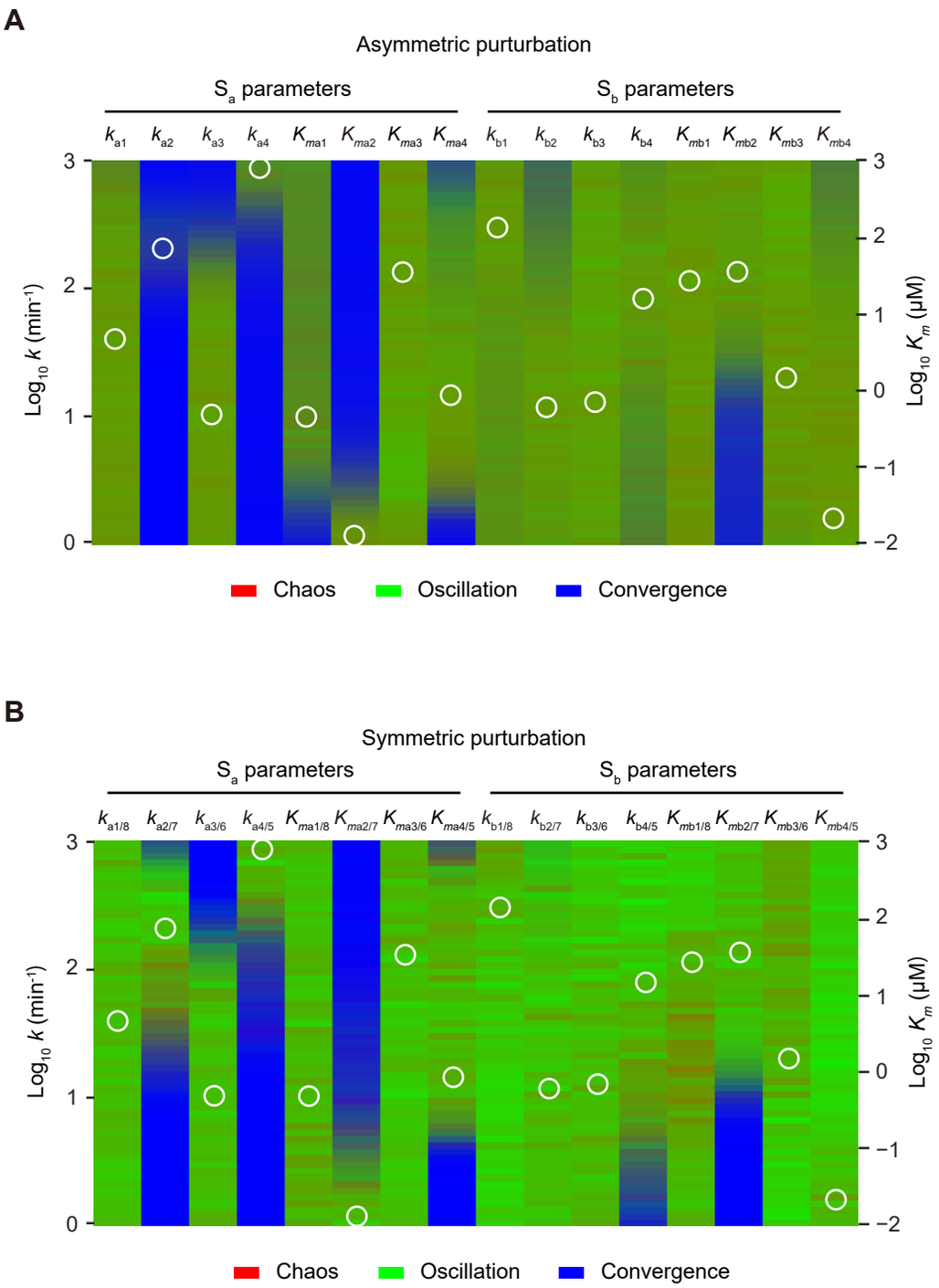

Figure S4. Yamaguchi et al.

Figure S4. Bifurcation analysis of stereotypical oscillation parameter sets.

(A) Bifurcation analysis was conducted for stereotypical oscillatory parameter sets (n = 97), all of which preserve the motif arrangement shown in the schematic representation in (A). The method used is same as that reported in **Figure 4B**.

(B) The same analysis as that in (A) is shown, except that the indicated parameter and its symmetrical pair (e.g., k_{a1} and k_{a8}, K_{mb4} and K_{mb5}) are simultaneously fixed to an indicated value.

See also **Figure 4**.

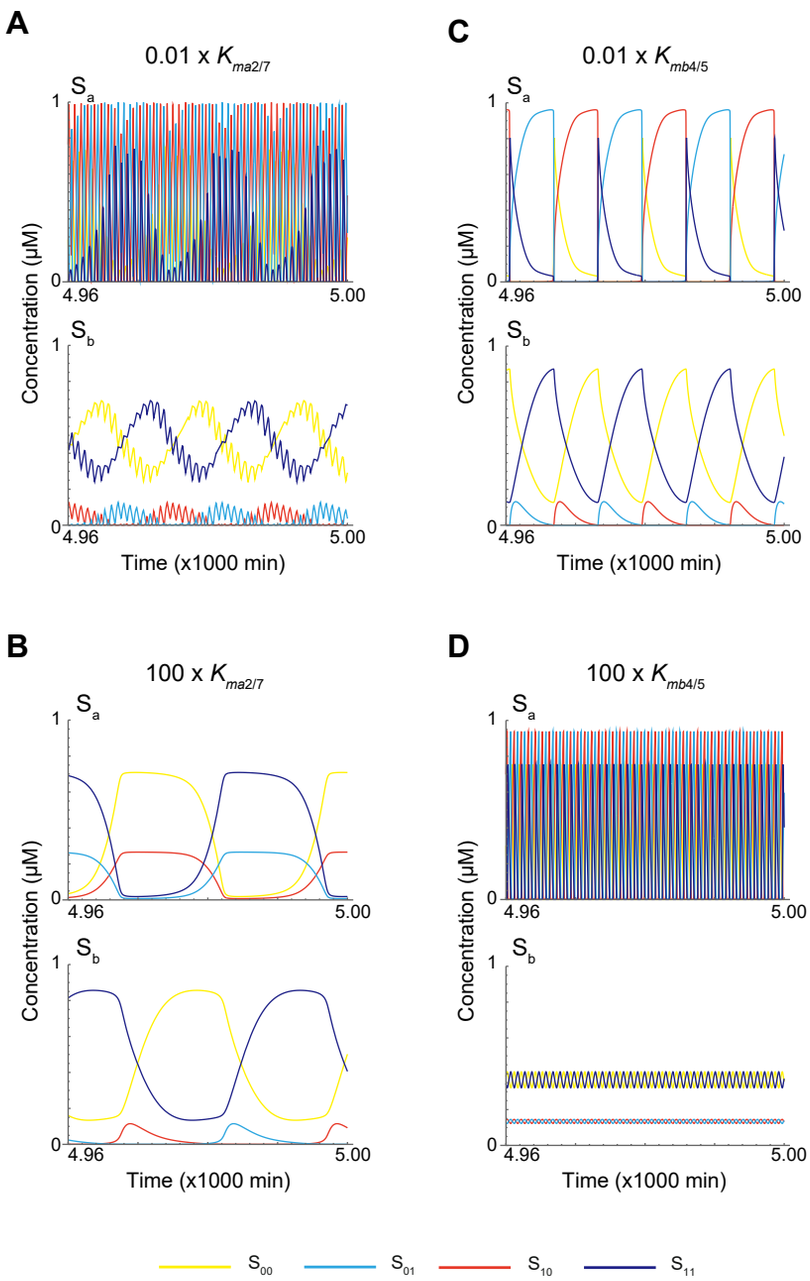

Figure S5. Yamaguchi et al.

Figure S5. Roles of enzyme trap efficiency in the coupling of two oscillators

(A, B) Time course of oscillatory dynamics for the representative parameter set with a 0.01-fold decrease (A) or 100-fold increase (B) in the parameter values for symmetrical K_{ma2} and K_{ma7}. Increasing the enzyme sequestration efficiency by S_a substrate (A) did not severely affect chaotic dynamics; reducing the enzyme sequestration by S_a (B) only allowed S_b-sequestration to drive the rhythmic synchronization of phosphorylation states such that the entire dynamics became dominated by slow-frequency oscillation.

(C, D) Time course of oscillatory dynamics for the representative parameter set with a 0.01-fold decrease (C) or 100-fold increase (D) in the parameter values for symmetrical K_{mb4} and K_{mb5}. Increasing the enzyme sequestration efficiency by S_b substrate (C) masked the high-frequency rhythmicity driven by S_a; reducing the enzyme sequestration by S_b (D) only allowed S_a-sequestration to drive the rhythmic synchronization of phosphorylation states such that the entire dynamics became dominated by high-frequency oscillation.

Supplemental Tables

Table S1. Example stereotypical chaos parameter set, related to **Figure 5**.

Parameter k (min^{-1}), K_m (μM)	Example stereotypical chaos parameter set
k_{a1}	47.24854606
k_{a2}	103.9531911
k_{a3}	10.08171512
k_{a4}	1060.571158
k_{a5}	1060.571158
k_{a6}	10.08171512
k_{a7}	103.9531911
k_{a8}	47.24854606
K_{ma1}	1.471248283
K_{ma2}	0.008378714
K_{ma3}	57.41102352
K_{ma4}	2.597629575
K_{ma5}	2.597629575
K_{ma6}	57.41102352
K_{ma7}	0.008378714
K_{ma8}	1.471248283
k_{b1}	209.3650037
k_{b2}	10.6326728
k_{b3}	19.66831864
k_{b4}	12.42448634
k_{b5}	12.42448634
k_{b6}	19.66831864
k_{b7}	10.6326728
k_{b8}	209.3650037
K_{mb1}	87.77317768
K_{mb2}	38.41198729
K_{mb3}	4.314899945
K_{mb4}	0.04746365
K_{mb5}	0.04746365
K_{mb6}	4.314899945
K_{mb7}	38.41198729
K_{mb8}	87.77317768

Table S2. Example stereotypical chaos parameter set for stochastic simulation, related to **Figure 5**.

Parameter k (min^{-1}), k_c (min^{-1} μM^{-1}), k_{uc} (min^{-1})	Example stereotypical chaos parameter set (stochastic simulation)
k_{a1}	47.24854606
k_{a2}	103.9531911
k_{a3}	10.08171512
k_{a4}	1060.571158
k_{a5}	1060.571158
k_{a6}	10.08171512
k_{a7}	103.9531911
k_{a8}	47.24854606
k_{uca1} - k_{uca8}	10
k_{ca1}	32.794
k_{ca2}	12526
k_{ca3}	0.19302
k_{ca4}	408.67
k_{ca5}	408.67
k_{ca6}	0.19302
k_{ca7}	12526
k_{ca8}	32.794
k_{b1}	209.3650037
k_{b2}	10.6326728
k_{b3}	19.66831864
k_{b4}	12.42448634
k_{b5}	12.42448634
k_{b6}	19.66831864
k_{b7}	10.6326728
k_{b8}	209.3650037
k_{ucb1} - k_{ucb8}	10
k_{cb1}	2.3967
k_{cb2}	0.30284
k_{cb3}	4.79
k_{cb4}	282.84
k_{cb5}	282.84
k_{cb6}	4.79
k_{cb7}	0.30284
k_{cb8}	2.3967

Transparent Methods

Modeling of coupled-posttranslational oscillator system

The coupled-posttranslational oscillator system was formulated as a set of ten ordinary differential equations that describe the temporal evolution of the concentrations of eight substrate phosphorylation states and two unbound enzymes.

$$\frac{\mathrm{d}[\mathrm{S_{a00}}]}{\mathrm{d}t} = -\left(\frac{k_{a1}}{K_{ma1}} + \frac{k_{a2}}{K_{ma2}}\right)[\mathrm{E}][\mathrm{S_{a00}}] + \left(\frac{k_{a5}}{K_{ma5}}[\mathrm{S_{a01}}] + \frac{k_{a6}}{K_{ma6}}[\mathrm{S_{a10}}]\right)[\mathrm{F}] \quad (1)$$

$$\frac{\mathrm{d}[\mathrm{S_{a01}}]}{\mathrm{d}t} = \left(\frac{k_{a1}}{K_{ma1}}[\mathrm{S_{a00}}] - \frac{k_{a3}}{K_{ma3}}[\mathrm{S_{a01}}]\right)[\mathrm{E}] + \left(-\frac{k_{a5}}{K_{ma5}}[\mathrm{S_{a01}}] + \frac{k_{a7}}{K_{ma7}}[\mathrm{S_{a11}}]\right)[\mathrm{F}] \quad (2)$$

$$\frac{\mathrm{d}[\mathrm{S_{a10}}]}{\mathrm{d}t} = \left(\frac{k_{a2}}{K_{ma2}}[\mathrm{S_{a00}}] - \frac{k_{a4}}{K_{ma4}}[\mathrm{S_{a10}}]\right)[\mathrm{E}] + \left(-\frac{k_{a6}}{K_{ma6}}[\mathrm{S_{a10}}] + \frac{k_{a8}}{K_{ma8}}[\mathrm{S_{a11}}]\right)[\mathrm{F}] \quad (3)$$

$$\frac{\mathrm{d}[\mathrm{S_{a11}}]}{\mathrm{d}t} = \left(\frac{k_{a3}}{K_{ma3}}[\mathrm{S_{a01}}] + \frac{k_{a4}}{K_{ma4}}[\mathrm{S_{a10}}]\right)[\mathrm{E}] - \left(\frac{k_{a6}}{K_{ma6}} + \frac{k_{a8}}{K_{ma8}}\right)[\mathrm{F}][\mathrm{S_{a11}}] \quad (4)$$

$$\frac{\mathrm{d}[\mathrm{S_{b00}}]}{\mathrm{d}t} = -\left(\frac{k_{b1}}{K_{mb1}} + \frac{k_{b2}}{K_{mb2}}\right)[\mathrm{E}][\mathrm{S_{b00}}] + \left(\frac{k_{b5}}{K_{mb5}}[\mathrm{S_{b01}}] + \frac{k_{b6}}{K_{mb6}}[\mathrm{S_{b10}}]\right)[\mathrm{F}] \quad (5)$$

$$\frac{\mathrm{d}[\mathrm{S_{b01}}]}{\mathrm{d}t} = \left(\frac{k_{b1}}{K_{mb1}}[\mathrm{S_{b00}}] - \frac{k_{b3}}{K_{mb3}}[\mathrm{S_{b01}}]\right)[\mathrm{E}] + \left(-\frac{k_{b5}}{K_{mb5}}[\mathrm{S_{b01}}] + \frac{k_{b7}}{K_{mb7}}[\mathrm{S_{b11}}]\right)[\mathrm{F}] \quad (6)$$

$$\frac{\mathrm{d}[\mathrm{S_{b10}}]}{\mathrm{d}t} = \left(\frac{k_{b2}}{K_{mb2}}[\mathrm{S_{b00}}] - \frac{k_{b4}}{K_{mb4}}[\mathrm{S_{b10}}]\right)[\mathrm{E}] + \left(-\frac{k_{b6}}{K_{mb6}}[\mathrm{S_{b10}}] + \frac{k_{b8}}{K_{mb8}}[\mathrm{S_{b11}}]\right) \quad (7)$$

$$\frac{\mathrm{d}[\mathrm{S_{b11}}]}{\mathrm{d}t} = \left(\frac{k_{b3}}{K_{mb3}}[\mathrm{S_{b01}}] + \frac{k_{b4}}{K_{mb4}}[\mathrm{S_{b10}}]\right)[\mathrm{E}] - \left(\frac{k_{b6}}{K_{mb6}} + \frac{k_{b8}}{K_{mb8}}\right)[\mathrm{F}][\mathrm{S_{b11}}] \quad (8)$$

$$[\mathrm{E}] = \frac{E_{\mathrm{total}}}{1 + \frac{[\mathrm{S_{a00}}]}{K_{ma1}} + \frac{[\mathrm{S_{a00}}]}{K_{ma2}} + \frac{[\mathrm{S_{a01}}]}{K_{ma3}} + \frac{[\mathrm{S_{a10}}]}{K_{ma4}} + \frac{[\mathrm{S_{b00}}]}{K_{mb1}} + \frac{[\mathrm{S_{b01}}]}{K_{mb2}} + \frac{[\mathrm{S_{b10}}]}{K_{mb3}} + \frac{[\mathrm{S_{b10}}]}{K_{mb4}}} \quad (9)$$

$$[\mathrm{F}] = \frac{F_{\mathrm{total}}}{1 + \frac{[\mathrm{S_{a01}}]}{K_{ma5}} + \frac{[\mathrm{S_{a10}}]}{K_{ma6}} + \frac{[\mathrm{S_{a11}}]}{K_{ma7}} + \frac{[\mathrm{S_{a11}}]}{K_{ma8}} + \frac{[\mathrm{S_{b01}}]}{K_{mb5}} + \frac{[\mathrm{S_{b10}}]}{K_{mb6}} + \frac{[\mathrm{S_{b11}}]}{K_{mb7}} + \frac{[\mathrm{S_{b11}}]}{K_{mb8}}} \quad (10)$$

In these equations, $[\mathrm{S_{a00}}]$, $[\mathrm{S_{a01}}]$, $[\mathrm{S_{a10}}]$, and $[\mathrm{S_{a11}}]$ represent the concentrations of the four phosphorylation states of substrate A; $[\mathrm{S_{b00}}]$, $[\mathrm{S_{b01}}]$, $[\mathrm{S_{b10}}]$, and $[\mathrm{S_{b11}}]$ represent the concentrations of the four phosphorylation states of substrate B; [E] and [F] are the concentrations of free (unbound) kinase and phosphatase; k_{a1}-k_{a8} and k_{b1}-k_{b8} are the reaction rate constants; K_{ma1}-K_{ma8} and K_{mb1}-K_{mb8} are the Michaelis−Menten constants; and E_{total} and F_{total} are the total concentrations of kinase and phosphatase.

Random parameter search for chaotic and oscillatory parameter sets

We randomly generated parameter sets that consisted of 32 constants (16 reaction rate constants and 16 Michaelis−Menten constants) and then numerically solved the equations to find chaotic parameter sets. Reaction rate constants k_{a1}-k_{a8} and k_{b1}-k_{b8} were independently generated from exponential distributions bounded between 1 and 1000 $\mathrm{min^{-1}}$. Michaelis−Menten constants K_{ma1}-K_{ma8} and K_{mb1}-K_{mb8} were independently generated from exponential distributions bounded between

0.01 and 1000 μM. The integration began from a state in which all the substrate molecules were dephosphorylated and all the enzyme molecules were unbounded ($[S_{a00}] = [S_{b00}] = 1000$ μM; [E] = [F] = 20 μM). The solution for each parameter set could be convergent, oscillatory, or chaotic. We judged a solution to be chaotic when its power spectrum was continuous rather than discrete; the spectrum was firstly numerically classified as not discrete if the proportion of the power at the peak frequency to the total power was below 15%. Then we plotted those candidate continuous spectrums and visually checked their continuity. We further checked the chaotic parameter sets to ensure that, after sufficient time had passed (t = 5000 min), the solution was divergent because of small changes in the initial state of the integration. The degree of divergence is visually inspected. Oscillatory parameter sets were collected in the same manner as chaotic parameter sets. Solutions were considered to be oscillatory when the power spectrum was discrete.

Clustering of chaotic parameter sets

Chaotic parameter sets collected in the random parameter search were standardized and clustered by performing a clustering analysis. In the standardization procedure, each constant was transformed so that the defined lower bound, upper bound, and the midpoint between them mapped to −1, 1, and 0, respectively. To achieve this, reaction rate constants were log-transformed with base 10, 1.5 was subtracted from the value [= (0 + 3)/2], and then this value was divided by 1.5 [= (3 − 0)/2]. Michaelis−Menten constants were log-transformed with base 10, 0.5 was subtracted from the value [= (3 + (−2))/2], and then this value was divided by 2.5 [= (3 − (−2))/2]. In the clustering analysis, standardized parameters were hierarchically clustered using Ward's algorithm. We used a special distance metric for the algorithm to consider the three symmetries of the system. These symmetries existed (1) in the phosphorylation states of each substrate (i.e., exchanging the position of S_{a01} and S_{a10}, or exchanging the position of S_{b01} and S_{b10}, conserves the overall structure), (2) as an enzymatic symmetry (i.e., exchanging the role of kinase and phosphatase conserves the overall structure), and (3) as a substrate symmetry (i.e., exchanging S_a and S_b conserves the overall structure). By considering the first symmetry, the parameter set that exchanged parameter {k_{a1}, K_{ma1}, k_{a2}, K_{ma2}, k_{a3}, K_{ma3}, k_{a4}, K_{ma4}, k_{a5}, K_{ma5}, k_{a6}, K_{ma6}, k_{a7}, K_{ma7}, k_{a8}, K_{ma8}} with {k_{a2}, K_{ma2}, k_{a1}, K_{ma1}, k_{a4}, K_{ma4}, k_{a3}, K_{ma3}, k_{a6}, K_{ma6}, k_{a5}, K_{ma5}, k_{a8}, K_{ma8}, k_{a7}, K_{ma7}} can be regarded as the same as the original set. Similarly, by considering the second symmetry, the parameter set that exchanged parameter {k_{a1}, K_{ma1}, k_{a2}, K_{ma2}, k_{a3}, K_{ma3}, k_{a4}, K_{ma4}, k_{a5}, K_{ma5}, k_{a6}, K_{ma6}, k_{a7}, K_{ma7}, k_{a8}, $K_{ma8,}$ k_{b1}, K_{mb1}, k_{b2}, K_{mb2}, k_{b3}, K_{mb3}, k_{b4}, K_{mb4}, k_{b5}, K_{mb5}, k_{b6}, K_{mb6}, k_{b7}, K_{mb7}, k_{b8}, K_{mb8}} with {k_{b7}, K_{mb7}, k_{b8}, K_{mb8}, k_{b5}, K_{mb5}, k_{b6}, K_{mb6}, k_{b3}, K_{mb3}, k_{b4}, K_{mb4}, k_{b1}, K_{mb1}, k_{b2}, $K_{mb2,}$ k_{b7}, K_{mb7}, k_{b8}, K_{mb8}, k_{b5}, K_{mb5}, k_{b6}, K_{mb6}, k_{b3}, K_{mb3}, k_{b4}, K_{mb4}, k_{b1}, K_{mb1}, k_{b2}, K_{mb2}} can be regarded as the same set. By considering the third symmetry, the parameter set that exchanged parameter {k_{a1}, K_{ma1}, k_{a2}, K_{ma2}, k_{a3}, K_{ma3}, k_{a4}, K_{ma4}, k_{a5}, K_{ma5}, k_{a6}, K_{ma6}, k_{a7}, K_{ma7}, k_{a8}, $K_{ma8,}$ k_{b1}, K_{mb1}, k_{b2}, K_{mb2}, k_{b3}, K_{mb3}, k_{b4}, K_{mb4}, k_{b5}, K_{mb5}, k_{b6}, K_{mb6}, k_{b7}, K_{mb7}, k_{b8}, K_{ma8}} with {k_{b1}, K_{mb1}, k_{b2}, K_{mb2}, k_{b3}, K_{mb3}, k_{b4}, K_{mb4}, k_{b5}, K_{mb5}, k_{b6}, K_{mb6}, k_{b7}, K_{mb7}, k_{b8}, $K_{mb8,}$ k_{a1}, K_{ma1}, k_{a2}, K_{ma2}, k_{a3}, K_{ma3}, k_{a4}, K_{ma4}, k_{a5}, K_{ma5}, k_{a6}, K_{ma6}, k_{a7}, K_{ma7}, k_{a8}, K_{ma8}} can be regarded as the same set. Given

these symmetries, the distance between two parameter sets P_1 and P_2 is defined as the minimum of the distances between P_1 and all the symmetrically exchangeable parameter sets of P_2. To abstract the motif structure, parameter histograms were calculated for each cluster. When observing the distribution of all parameters in all clusters (**Figures 2 and S2**), the highest frequency at which parameters occurred with highly skewed distributions was ~0.4. Therefore, we set a threshold value of 0.2, i.e., half the highest frequency.

Biased parameter search

Parameter sets were generated by introducing some specific biases to some of their parameters; the solutions were then classified in the same manner as for the random parameter search based on the power spectrum. The biases were determined as combinations of motif A bias and motif B bias. Both motif A bias and motif B bias consisted of two biased parameters, one for a high reaction rate constant and the other for a low Michaelis−Menten constant. When the bias for the reaction rate constant was set, the parameter was randomly generated from an exponential distribution bounded between 100 and 1000 min^{-1}. When the bias for the Michaelis−Menten constant was set, the parameter was randomly generated from an exponential distribution bounded between 0.01 and 0.1 μM. In this biased parameter search, we did not apply visual inspection of the sentisitivity to initial conditions. The lack of this confirmation would not critically deteriorate the classification performance for a chaos parameter set: for a follow-up analysis, we randomly chose 1,000 parameter sets that were classified as chaos through all the biased conditions and inspected their sensitivity to initial conditions. Through the inspection, only 12 parameters were found to be misclassified (in other words, 98.8% of chaos parameters were accurately classified as chaos without the visual inspection of initial condition sensitivity).

Collection of stereotypical chaos and oscillatory parameter sets

To obtain stereotypical chaos parameter sets with symmetrical structures, we used the results of the biased parameter search corresponding to motif arrangement #46. Parameters were randomly sampled from a Gaussian distribution defined by the mean and the covariance matrix of chaos parameters obtained from the biased parameter search. In this sampling, distributions were not bounded within a specific range. The sampled parameter was modified so that it had a symmetrical structure, i.e., $k_{ai} = k_{a(9-i)}$, $k_{bi} = k_{b(9-i)}$, $K_{mai} = K_{ma(9-i)}$, $K_{mbi} = K_{mb(9-i)}$ for i = 1…4. The solution was then determined to be either chaotic or not chaotic as described in the method section “Random parameter search for chaotic and oscillatory parameter sets”. In total, 97 chaotic parameters were collected from 10 million random sampling repeats. Chaotic parameters were confirmed to show initial condition sensitivity. The stereotypical oscillatory parameter sets were obtained by the same procedure except that the numerical solution was considered to be oscillation. Collection of oscillatory parameter sets continued until 97 sets were found.

The example chaos parameter set was selected as follows. Each stereotypical chaos

parameter set was first standardized, which was conducted using the same method described for the clustering procedure. The example parameter set was then selected as the one closest to the mean of the standardized parameter sets. The distance between parameter sets was measured by Euclidian distance. The values of the selected stereotypical chaos parameter sets are shown in **Table S1**.

Bifurcation analysis

Each parameter in the typical chaotic parameter set varied between the following ranges: 1 and 1000 min^{-1} for the reaction rate constant; 0.01 and 0.1 μM for the binding constant. The varied value took 30 logarithmically-spaced points between the ranges, including both sides. For each analysis, the solution type was determined as as described in the method section “Random parameter search for chaotic and oscillatory parameter sets”. For asymmetric perturbation, when bifurcation analysis on each specific parameter had been conducted, the other parameters at the symmetrical positions were fixed to the original value, resulting in a violation of symmetry. For symmetric perturbation, both parameters at the symmetrical positions (e.g., k_{a1} and k_{a8}) varied simultaneously. Bifurcation maps were produced based on the results of the bifurcation analysis. The color of each cell was specified using a RGB color code: the R channel was set to the proportion of chaos behavior, G was the proportion of oscillation, and B was the proportion of convergence.

Stochastic simulation

The stochastic simulation was performed using Gillespie’s direct method stochastic simulation algorithm implemented in StochPy (Maarleveld et al., 2013). We modified the simulation to track the behavior of the full system including each kinase−substrate complex molecule. The full ordinary differential equation system, without application of the Michaelis−Menten approximation, is described below.

$$\frac{\mathrm{d}[\mathrm{S_{a00}}]}{\mathrm{d}t} = -(k_{ca1} + k_{ca2})[\mathrm{E}][\mathrm{S_{a00}}] + k_{uca1}[\mathrm{ES_{a00\rightarrow a01}}] + k_{uca2}[\mathrm{ES_{a00\rightarrow a10}}] + k_{a5}[\mathrm{FS_{a01}}] + k_{a6}[\mathrm{FS_{a10}}] \quad (11)$$

$$\frac{\mathrm{d}[\mathrm{S_{a01}}]}{\mathrm{d}t} = -k_{ca3}[\mathrm{E}][\mathrm{S_{a01}}] + k_{uca3}[\mathrm{ES_{a01}}] - k_{ca5}[\mathrm{F}][\mathrm{S_{a01}}] + k_{uca5}[\mathrm{FS_{a01}}] + k_{a1}[\mathrm{ES_{a00\rightarrow a01}}] + k_{a7}[\mathrm{FS_{a11\rightarrow a01}}] \quad (12)$$

$$\frac{\mathrm{d}[\mathrm{S_{a10}}]}{\mathrm{d}t} = -k_{ca4}[\mathrm{E}][\mathrm{S_{a10}}] + k_{uca4}[\mathrm{ES_{a10}}] - k_{ca6}[\mathrm{F}][\mathrm{S_{a10}}] + k_{uca6}[\mathrm{FS_{a10}}] + k_{a2}[\mathrm{ES_{a00\rightarrow a10}}] + k_{a8}[\mathrm{FS_{a11\rightarrow a10}}] \quad (13)$$

$$\frac{\mathrm{d}[\mathrm{S_{a11}}]}{\mathrm{d}t} = -(k_{ca7} + k_{ca8})[\mathrm{F}][\mathrm{S_{a11}}] + k_{uca7}[\mathrm{FS_{a11\rightarrow a01}}] + k_{uca8}[\mathrm{FS_{a11\rightarrow a10}}] + k_{a3}[\mathrm{ES_{a01}}] + k_{a4}[\mathrm{ES_{a10}}] \quad (14)$$

$$\frac{\mathrm{d}[\mathrm{ES_{a00\rightarrow a01}}]}{\mathrm{d}t} = k_{ca1}[\mathrm{E}][\mathrm{S_{a00}}] - (k_{uca1} + k_{a1})[\mathrm{ES_{a00\rightarrow a01}}] \quad (15)$$

$$\frac{\mathrm{d}[\mathrm{ES_{a00\rightarrow a10}}]}{\mathrm{d}t} = k_{ca2}[\mathrm{E}][\mathrm{S_{a00}}] - (k_{uca2} + k_{a2})[\mathrm{ES_{a00\rightarrow a10}}] \tag{16}$$

$$\frac{\mathrm{d}[\mathrm{ES_{a01}}]}{\mathrm{d}t} = k_{ca3}[\mathrm{E}][\mathrm{S_{a01}}] - (k_{uca3} + k_{a3})[\mathrm{ES_{a01}}] \tag{17}$$

$$\frac{\mathrm{d}[\mathrm{ES_{a10}}]}{\mathrm{d}t} = k_{ca4}[\mathrm{E}][\mathrm{S_{a10}}] - (k_{uca4} + k_{a4})[\mathrm{ES_{a10}}] \tag{18}$$

$$\frac{\mathrm{d}[\mathrm{FS_{a01}}]}{\mathrm{d}t} = k_{ca5}[\mathrm{F}][\mathrm{S_{a01}}] - (k_{uca5} + k_{a5})[\mathrm{FS_{a01}}] \tag{19}$$

$$\frac{\mathrm{d}[\mathrm{FS_{a10}}]}{\mathrm{d}t} = k_{ca6}[\mathrm{F}][\mathrm{S_{a10}}] - (k_{uca6} + k_{a6})[\mathrm{FS_{a10}}] \tag{20}$$

$$\frac{\mathrm{d}[\mathrm{FS_{a11\rightarrow a01}}]}{\mathrm{d}t} = k_{ca7}[\mathrm{F}][\mathrm{S_{a11}}] - (k_{uca7} + k_{a7})[\mathrm{FS_{a11\rightarrow a01}}] \tag{21}$$

$$\frac{\mathrm{d}[\mathrm{FS_{a11\rightarrow a10}}]}{\mathrm{d}t} = k_{ca8}[\mathrm{F}][\mathrm{S_{a11}}] - (k_{uca8} + k_{a8})[\mathrm{FS_{a11\rightarrow a10}}] \tag{22}$$

$$\frac{\mathrm{d}[\mathrm{S_{b00}}]}{\mathrm{d}t} = -(k_{cb1} + k_{cb2})[\mathrm{E}][\mathrm{S_{b00}}] + k_{ucb1}[\mathrm{ES_{b00\rightarrow b01}}] + k_{ucb2}[\mathrm{ES_{b00\rightarrow b10}}] + k_{b5}[\mathrm{FS_{b01}}] + k_{b6}[\mathrm{FS_{b10}}] \tag{23}$$

$$\frac{\mathrm{d}[\mathrm{S_{b01}}]}{\mathrm{d}t} = -k_{cb3}[\mathrm{E}][\mathrm{S_{b01}}] + k_{ucb3}[\mathrm{ES_{b01}}] - k_{cb5}[\mathrm{F}][\mathrm{S_{b01}}] + k_{ucb5}[\mathrm{FS_{b01}}] + k_{b1}[\mathrm{ES_{b00\rightarrow b01}}] + k_{b7}[\mathrm{FS_{b11\rightarrow b01}}] \tag{24}$$

$$\frac{\mathrm{d}[\mathrm{S_{b10}}]}{\mathrm{d}t} = -k_{cb4}[\mathrm{E}][\mathrm{S_{b10}}] + k_{ucb4}[\mathrm{ES_{b10}}] - k_{cb6}[\mathrm{F}][\mathrm{S_{b10}}] + k_{ucb6}[\mathrm{FS_{b10}}] + k_{b2}[\mathrm{ES_{b00\rightarrow b10}}] + k_{b8}[\mathrm{FS_{b11\rightarrow b10}}] \tag{25}$$

$$\frac{\mathrm{d}[\mathrm{S_{b11}}]}{\mathrm{d}t} = -(k_{cb7} + k_{cb8})[\mathrm{F}][\mathrm{S_{b11}}] + k_{ucb7}[\mathrm{FS_{b11\rightarrow b01}}] + k_{ucb8}[\mathrm{FS_{b11\rightarrow b10}}] + k_{b3}[\mathrm{ES_{b01}}] + k_{b4}[\mathrm{ES_{b10}}] \tag{26}$$

$$\frac{\mathrm{d}[\mathrm{ES_{b00\rightarrow b01}}]}{\mathrm{d}t} = k_{cb1}[\mathrm{E}][\mathrm{S_{b00}}] - (k_{ucb1} + k_{b1})[\mathrm{ES_{b00\rightarrow b01}}] \tag{28}$$

$$\frac{\mathrm{d}[\mathrm{ES_{b00\rightarrow b10}}]}{\mathrm{d}t} = k_{cb2}[\mathrm{E}][\mathrm{S_{b00}}] - (k_{ucb2} + k_{b2})[\mathrm{ES_{b00-b10}}] \tag{29}$$

$$\frac{\mathrm{d}[\mathrm{ES_{b01}}]}{\mathrm{d}t} = k_{cb3}[\mathrm{E}][\mathrm{S_{b01}}] - (k_{ucb3} + k_{b3})[\mathrm{ES_{b01}}] \tag{30}$$

$$\frac{\mathrm{d}[\mathrm{ES_{b10}}]}{\mathrm{d}t} = k_{cb4}[\mathrm{E}][\mathrm{S_{b10}}] - (k_{ucb4} + k_{b4})[\mathrm{ES_{b10}}] \tag{31}$$

$$\frac{\mathrm{d}[\mathrm{FS_{b01}}]}{\mathrm{d}t} = k_{cb5}[\mathrm{F}][\mathrm{S_{b01}}] - (k_{ucb5} + k_{b5})[\mathrm{FS_{b01}}] \tag{32}$$

$$\frac{\mathrm{d}[\mathrm{FS_{b10}}]}{\mathrm{d}t} = k_{cb6}[\mathrm{F}][\mathrm{S_{b10}}] - (k_{ucb6} + k_{b6})[\mathrm{FS_{b10}}] \tag{33}$$

$$\frac{\mathrm{d}[\mathrm{FS_{b11\rightarrow b01}}]}{\mathrm{d}t} = k_{cb7}[\mathrm{F}][\mathrm{S_{b11}}] - (k_{ucb7} + k_{b7})[\mathrm{FS_{b11\rightarrow b01}}] \tag{34}$$

$$\frac{\mathrm{d}[\mathrm{FS_{b11\rightarrow b10}}]}{\mathrm{d}t} = k_{cb8}[\mathrm{F}][\mathrm{S_{b11}}] - (k_{ucb8} + k_{b8})[\mathrm{FS_{b11\rightarrow b10}}] \tag{35}$$

$$\frac{\mathrm{d[E]}}{\mathrm{d}t} = -\big((k_{ca1} + k_{ca2})[\mathrm{S_{a00}}] + k_{ca3}[\mathrm{S_{a01}}] + k_{ca4}[\mathrm{S_{a10}}]\big)[\mathrm{E}] + (k_{uca1} + k_{a1})[\mathrm{ES_{a00\to a10}}] + (k_{uca2} + k_{a2})[\mathrm{ES_{a00\to a10}}] + (k_{uca3} + k_{a3})[\mathrm{ES_{a01}}] + (k_{uca4} + k_{a4})[\mathrm{ES_{a10}}] - \big((k_{cb1} + k_{cb2})[\mathrm{S_{b00}}] + k_{cb3}[\mathrm{S_{b01}}] + k_{cb4}[\mathrm{S_{b10}}]\big)[\mathrm{E}] + (k_{ucb1} + k_{b1})[\mathrm{ES_{b00\to b01}}] + (k_{ucb2} + k_{b2})[\mathrm{ES_{b00\to b10}}] + (k_{ucb3} + k_{b3})[\mathrm{ES_{b01}}] + (k_{ucb4} + k_{b4})[\mathrm{ES_{b10}}] \quad (36)$$

$$\frac{\mathrm{d[F]}}{\mathrm{d}t} = -(k_{ca5}[\mathrm{S_{a00}}] + k_{ca6}[\mathrm{S_{a10}}] + (k_{ca7} + k_{ca8})[\mathrm{S_{a11}}])[\mathrm{F}] + (k_{uca5} + k_{a5})[\mathrm{FS_{01}}] + (k_{uca6} + k_{a6})[\mathrm{FS_{a10}}] + (k_{uca7} + k_{a7})[\mathrm{FS_{a11\to a01}}] + (k_{uca8} + k_{a8})[\mathrm{FS_{a11\to a10}}] - (k_{cb5}[\mathrm{S_{b00}}] + k_{cb6}[\mathrm{S_{b10}}] + (k_{cb7} + k_{cb8})[\mathrm{S_{b11}}])[\mathrm{F}] + (k_{ucb5} + k_{b5})[\mathrm{FS_{01}}] + (k_{ucb6} + k_{b6})[\mathrm{FS_{b10}}] + (k_{ucb7} + k_{b7})[\mathrm{FS_{b11\to b01}}] + (k_{ucb8} + k_{b8})[\mathrm{FS_{b11\to b10}}] \quad (37)$$

In these equations, [S_{a00}], [S_{a01}], [S_{a10}], and [S_{a11}] represent the concentrations of the four phosphorylation states of substrate A; [S_{b00}], [S_{b01}], [S_{b10}], and [S_{b11}] represent the concentrations of the four phosphorylation states of substrate B; [E] and [F] are the concentrations of free (unbound) kinase and phosphatase; [ES] and [FS] are the enzyme-substrate complex concentrations with the arrow in the subscript indicating which reaction the complex is involved in (e.g., $ES_{a00\to a01}$ denotes that the ES complex is involved in the kinase reaction converting S_{a00} to S_{a01}); k_{a1}-k_{a8} and k_{b1}-k_{b8} are the catalytic rate constants; k_{ca1}-k_{ca8} and k_{cb1}-k_{cb8} are the binding constants; and k_{uca1}-k_{uca8} and k_{ucb1}-k_{ucb8} are the unbinding constants. The values of the parameter sets are shown in **Table S2**. The relationship among the Michaelis−-Menten constants, binding constants, and unbinding constants is described as follows:

$$K_{mi} = \frac{k_{uci} + k_i}{k_{ci}}, \text{for i} = 1 \ldots 8 \quad (38)$$

Software for computer simulation

Numerical integration and clustering were carried out by Python 3.6.1 with the libraries of numpy 1.12.1 and scipy 0.19.1, or by Mathematica 12.0 (Wolfram Research). Stochastic simulation was carried out by StochPy 2.3.